Optimizing the Illumination of a Surgical Site in New Autonomous Module-based Surgical Lighting Systems

Andre Mühlenbrock, René Weller, and Gabriel Zachmann

Faculty of Computer Science, University of Bremen, Germany
{muehlenb,weller,zach}@cs.uni-bremen.de

Abstract. Good illumination of the surgical site is crucial for the success of a surgery - yet current, typical surgical lighting systems have significant shortcomings, e.g. with regard to shadowing and ease of handling. To address these shortcomings, new lighting systems for operating rooms have recently been developed, consisting of a variety of swiveling light modules that are mounted on the ceiling and controlled automatically. For such a new type of lighting system, we present a new optimization pipeline that maintains the brightness at the surgical site as constant as possible over time and minimizes shadows by using depth sensors. Furthermore, by performing simulations on point cloud recordings of nine real abdominal surgeries, we demonstrate that our optimization pipeline is capable of effectively preventing shadows cast by bodies and heads of the OR personnel.

Keywords: surgical lighting, optimal illumination, depth sensors

1 Introduction

Although good illumination of the surgical site - i.e. the wound - is so important for the success of an operation, existing solutions, e.g. conventional surgical lighting system (SLS) or head lamps, have major disadvantages. In the case of SLS, the main drawback is the shadowing by OR personnel around the table that makes illumination of an OR wound difficult and requires frequent manual readjustments of the SLS. Head lamps, on the other hand, are strenuous to wear for long periods of time and require the wearer to assume a certain head posture.

To solve the problems of these SLS, new surgical lighting systems have been developed to automatically prevent shadows and to keep the brightness in the surgical site at the desired level constantly over time and as evenly distributed as possible over the area. These new surgical lighting systems do not consist of two or three conventional large lighting systems, but of a large number of small swiveling light modules placed at the ceiling that are automatically rotated and intensity-controlled with the aid of a central control computer. Recent examples

are the Optimus ISE Celestial™ Surgical Lighting System[1], and the lighting system developed in the SmartOT research project[2].

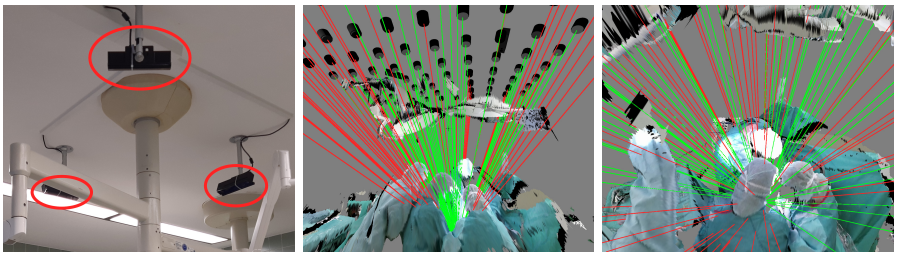

Fig. 1: Left: The Kinect cameras we used to record nine real open abdominal surgeries in an operating room. Center and right: The resulting point cloud recordings against which we can perform ray tests.

In this paper, we present a novel optimization pipeline for such lighting systems based on multiple depth sensors such as Microsoft's Kinect. By simulating the optimization with point cloud recordings of nine real open abdominal surgeries (see Figure 1), we compare different parameters and fitness scores with respect to the illumination they create at a virtual surgical site.

2 Related Work

In today's operating rooms, SLS are commonly used for traditional open surgery. However, they still come with some disadvantages: According to Knulst et al.[1], conventional surgical lights are readjusted every 7.5 minutes on average to provide appropriate illumination for the surgical site. In addition, surgeons and other OR personnel often saw a need for improvement in lighting intensity, shadowing, illumination of deep wounds, and the handling of such lights. Curlin et al. [2] also elaborates on the advantages and disadvantages of surgical lights and other common lighting systems, including head lights, lighted retractors, and operating microscopes, none of which meet all lighting needs.

As an approach to improve the handling of conventional SLS, Dietz et al. [3] suggest to use a gesture control for brightness and color temperature instead of using a control panel, which is usually located high up on the SLS. An attempt to also address the problem of manual repositioning and alignment of conventional surgical lights was provided by Teuber et al. [4], in which three motor-driven surgical lights automatically position themselves so that shadows are avoided. This optimization was further optimized in [5]. We have discussed developing these ideas further and implementing a similar motor-driven approach, but have

[1] See https://www.optimus-ise.com/
[2] See https://www.smart-ot.de/

rejected it due to several drawbacks, including the expected noise and the danger in terms of collisions with OR personnel.

In novel lighting concepts for operating rooms, as in the SmartOT project, a variety of small lighting modules are proposed that are placed on the ceiling and control themselves to automatically generate optimal illumination at the site and avoid shadowing. Recently, an optimization procedure was presented in [6] to position the light modules of such lighting systems on the ceiling with the help of point cloud recordings in such a way that the most satisfactory illumination is theoretically reachable during the entire surgery.

Nevertheless, to the best of our knowledge, methods to optimize the intensity of light modules at the runtime of the surgery for this new type of surgical lighting system have not been presented or evaluated in the literature up to this point.

3 Implementation

In this section, we present our optimization pipeline (Section 3.3) as well as the specific optimization of the intensities of individual light modules (Section 3.4). For understanding, we briefly discuss the different types of shadows beforehand in Section 3.1 and describe our surgical site model for enabling the illumination of deep wounds in Section 3.2.

3.1 Occluder Types

The shadows in surgeries can be divided into two categories: On the one hand, there are shadows caused by hands and OR instruments, where occluders – the hands and instruments – are very close to the site. These shadows are difficult to compensate for by an autonomous shadow management because the lights in question change very quickly due to the fast movements and the short distance of the occluder to the surgical site. The most time, even all the lights cast a shadow for these type of occluders. In new module-based lighting concepts, these shadows can be compensated by distributing as many light modules as possible over a large area which are used simultaneously.

On the other hand, there are shadows caused by the heads and bodies of OR personnel: for these type of occluders, only some lamps cast shadows at the surgical site simultaneously, since the head and body of individual persons are usually located to the side of the surgical site and their distance to the site is greater. In this section, we mainly focus on preventing this type of shadowing.

3.2 Representation of the Surgical Site

In order to illuminate narrow, deep surgical sites, the site is modeled using a virtual cylinder-shaped tube, which can be placed, rotated and scaled in diameter and depth. By not just testing for occlusions by the point cloud geometry but also against this tube, we can ensure that only light modules are used which are able to illuminate the site in depth when this is required. This virtual surgical site model is visualized in Figure 3.

3.3 Optimization Pipeline

Our pipeline (see Figure 2) starts with the depth images from multiple depth cameras as input. The cameras are placed on the ceiling between the lamps. By using the camera intrinsics and extrinsics parameters, a point cloud is generated in camera space, registered to each other and transformed into world space – in our case the OR room. In case of the point cloud recordings of the nine surgery used for evaluation, we used a lattice registration procedure [7] to extrinsically calibrate the depth cameras.

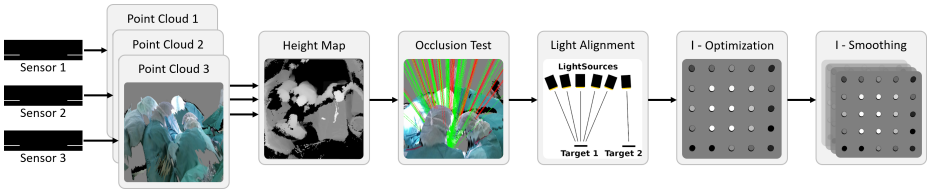

Fig. 2: The pipeline starts with the input of the depth sensors and ends with the output of the parameters to control the light modules, described in detail in Section 3.3.

In order to efficiently test for occlusions, we first transform the separate point clouds of multiple depth sensors into a common geometric datastructure, which is a height map that stores the height from the ground in the 2 m x 2 m area around the operating table. In a first step, we remove occlusions of the first type according to Section 3.1, i.e. hands and instruments close to the site. This can be easily achieved by simply removing all points of the point cloud within a fixed radius r around the site (we used $r = 0.3m$).

By projecting a ray into this height map and iterate over the resulting line, we can efficiently calculate for each light module whether there is an occluding object in the path that would lead to shadows at the site. To test whether a ray is blocked by the surgical site model (see Section 3.2), a simple ray-plane intersection test can be performed where the distance between the intersection point and plane midpoint is tested against the tube radius. By testing multiple rays per light module which are starting at different positions on the luminous surface and run to different positions in the site, we moreover calculate a floating point value v_i that indicates how much a light module i is blocked by the geometry. To reduce sensor noise, we filter this value using a 1D Kalman filter.

Next, the light modules in the pipeline are assigned to a light target and rotated accordingly so that they are aligned with it. This is done according to the desired setting defined by the OR staff. Finally the optimization and smoothing of the intensities of the light modules takes place which is described in Section 3.4.

3.4 Light Intensity Optimization

Requirements Since we want to optimize the intensity I^i of every light module i in such a way that the illuminance E_v at the surgical site is as constant as possible and close to the desired value $E_{v_{\text{Pref}}}$, we need be able to calculate what illumination E_v^{i} is produced by a single light module i at the site.

In order to be able to calculate which intensity values I^i produce which illumination E_v^i at the center of the site for any one of the modules of the light module array, we assume that for an arbitrary chosen, but fixed distance d_{Norm} and a perpendicular incidence of light, a mapping function f is known that maps the intensity I^i the light module i is driven with to illumination $E_{v_{\text{Norm}}}^{\text{i}}$:

$$E_{v_{\text{Norm}}}^{\text{i}} = f(I^i) \tag{1}$$

Given the distance d^i from a light module i to the center of the surgical site, the virtual site surface normal $\vec{n}$ and the light vector $\vec{l^i}$ of light module i, we approximate the luminance E_v^{i} as follows:

$$E_v^{\text{i}} = E_{v_{\text{Norm}}}^{\text{i}} \cdot (\frac{d_{\text{Norm}}}{d^i})^2 \cdot (-\vec{l^i} \cdot \vec{n}) \tag{2}$$

Note that we assume that the illuminance of the used light modules decreases approximately quadratically over distance. The term $(-\vec{l_i} \cdot \vec{n})$, on the other hand, describes the decrease in luminance when the surface on which the same amount of light is incident increases due to a tilt – similar to Lambert's cosine law.

***I*-Optimization** The optimization approach can be summarized by the following two steps: In the first step, the light modules are sorted according to their suitability to illuminate the site well. In the second step, each non-occluded light module is assigned a certain amount of light until the target brightness is reached, starting with the most suitable light module.

To sort the light modules, we implemented two different scores. The first score is the perpendicularity of the inverse light vector $-\vec{l}$ to the site surface with the surface normal $\vec{n}$:

$$s^i_{Perpendicular} = (-\vec{l_i} \cdot \vec{n}) \tag{3}$$

The second score we have implemented counts the number of last consecutive frames in which the floating-point number value v filtered with the 1D Kalman filter (see Section 3.3) was greater than 0.9:

$$s^i_{SuccessiveUnblocked} = \#\text{Consecutive frames with } v^i \geq 0.9 \tag{4}$$

After sorting the light modules by their presumed ability to illuminate the site well, we calculate the maximum illuminance $E_{v_{\text{Max}}}$ the system is able to provide at the center of the surgical site. To do this, we use a simple heuristic: The maximum illuminance $E^i_{v_{\text{Max}}}$ a light module i can produce at the center of

the site is multiplied by the relative number of unblocked light rays from that light module i to the site and then summed up over all light module:

$$E_{v_{\mathrm{Max}}} = \sum^{i} E^{i}_{v_{\mathrm{Max}}} \cdot \mathrm{unblockedRays}(i) \tag{5}$$

Before we iterate over the list of sorted light modules, we define the ratio which describes how much illuminance is preferred ($E_{v_{\mathrm{Pref}}}$) compared to the illuminance $E_{v_{\mathrm{Max}}}$ the system is actually able to provide using all unblocked light modules:

$$\omega = \min(1, \frac{E_{v_{\mathrm{Pref}}}}{E_{v_{\mathrm{Max}}}}) \tag{6}$$

In addition, we define a variable $E_{v_{\mathrm{Rem}}}$ that is decreased over time and describes which illuminance is still needed to reach the preferred illuminance $E_{v_{\mathrm{Pref}}}$. Accordingly, it is initialized with the preferred illuminance:

$$E_{v_{\mathrm{Rem}}} \leftarrow E_{v_{\mathrm{Pref}}} \tag{7}$$

Finally, we iterate over the list of sorted light modules and calculate the intensity I^i with which each light module i should be driven. In order to investigate how the number of simultaneous lights used affects the characteristics of the illumination, we have adapted our optimization method to be configurable by a floating-point light spread parameter α, which specifies whether as few optimal and unblocked light modules as possible should be used ($\alpha = 0.0$), or whether the desired brightness should be achieved by using all the unblocked light modules ($\alpha = 1.0$):

$$I^i = I^i_{\mathrm{Max}}(1 - \alpha) + I^i_{\mathrm{Max}} \cdot \omega \cdot \alpha \tag{8}$$

Moreover, we calculate the illuminance E^i_v expected to be achieved at the site for the light module i by using equation (1) and (2):

$$E^{\mathrm{i}}_v = f(I^i) \cdot (\frac{d_{\mathrm{Norm}}}{d_i})^2 \cdot (-\vec{l_i} \cdot \vec{n}) \tag{9}$$

In the case that this value E^{i}_v is lower that the remaining required illumination, i.e. $E^{\mathrm{i}}_v \leq E_{v_{\mathrm{Rem}}}$, the illumination of this light module i is subtracted from the remaining needed illumination:

$$E_{v_{\mathrm{Rem}}} \leftarrow E_{v_{\mathrm{Rem}}} - E^{\mathrm{i}}_v \tag{10}$$

In the case that the illumination of light module i would exceed the remaining needed illumination, i.e. $E^{\mathrm{i}}_v > E_{v_{\mathrm{Rem}}}$, we recalculate the intensity with which the light module should be driven:

$$I^i \leftarrow I^i \cdot \frac{E_{v_{\mathrm{Rem}}}}{E^i_v} \tag{11}$$

as well as we set the remaining needed illumination to zero and stop the iteration at that light. The intensity of all other light modules is left at zero.

***I*-Smoothing** Since we do not want the light to react immediately to every movement around the site, as this might distract surgeons, we perform a temporal smoothing of the intensity values I^i for every light i. We do this by simply blending the already smoothed intensities ${I_{Smoothed}}^{i,t-1}$ of the previous frame $t-1$ with the optimal luminous power $I^{i,t}$ of the current frame t by using a blending value $\gamma \in (0,1]$:

$$I^{i,t}_{\text{Smoothed}} = I^{i,t-1}_{\text{Smoothed}} \cdot (1-\gamma) + I^{i,t} \cdot \gamma \tag{12}$$

Remarks Currently, we shoot multiple rays from a single light module to different points at the surgical site to calculate the unblocked amount of light v_i for each light module i (see description of v_i in Section 3.3), but for intensity optimization, we only consider the illumination at a single point, i.e. the center of the surgical site. However, it would also be possible to optimize the illumination not only for a single point but for the whole surface area: This might be particularly useful if the emission characteristics of the light module are distributed unevenly over the surface (e.g. for cost reasons of the installed LED as seen in Figure 3).

Nevertheless, such an optimization causes some problems: On the one hand, currently, our site model is only very coarse, mainly, because of the limited resolution and the fixed viewing angle of the depth sensors that are not able to capture the complex geometry and details of real world sites. Moreover, the emission characteristics of the *actual physical light modules* – e.g. beam angle – cannot be changed. Consequently, the only way to compensate for uneven emission patterns remains the continuous rotation of the light modules.

But even if optimization over the entire area currently seems to make little sense due to these problems, our pipeline as a whole is prepared to handle this as we are able to estimate the illumination in multiple points at a site.

4 Results

In this section, we evaluate our optimization pipeline in a simulation on point cloud recordings of nine real abdominal surgeries. The methodology of the evaluation is presented in Section 4.1. Since the best possible light in the surgical situs is generally assumed to be (a) as free of shadows as possible and (b) should not change visibly as much as possible to avoid interference, we examine the quality of illumination with respect to these aspects in Sections 4.2 and 4.3.

4.1 Methods

For the evaluation, we used point cloud recordings of nine real abdominal surgeries taken at Pius-Hospital Oldenburg, Germany (see Figure 1). The setup of the evaluated virtual lighting system was as follows: We used 7 x 8 light modules at a height of 2.5 m arranged in a grid with a spacing of 36 cm x 35 cm. The preferred illumination $E_{v_{\text{Pref}}}$ was set to 80 klx. Single light modules were able to generate almost 50 klx at the site center at a distance of 1.9 m when driven at maximum intensity. We placed 5 x 5 sensors on an area of 5 cm x 5 cm in the

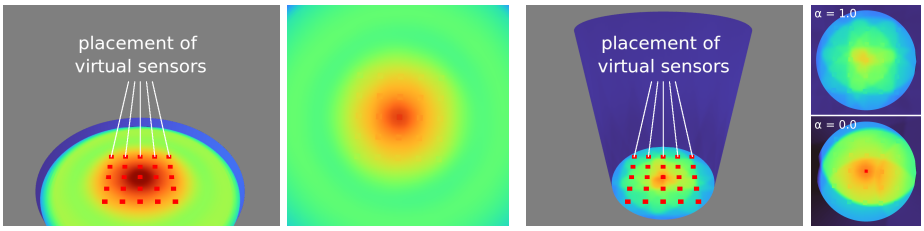

(a) Flat site (b) Deep site

Fig. 3: Visualization of the sensors placed onto (a) an almost flat surgical site and (b) a deep surgical site with a depth of 10 cm and a diameter of 7.5 cm. Here, the illumination is color coded using the Google turbo color map.

virtual site and simulated the brightness at 60 Hz using an illumination profile of the actual planned light modules in the SmartOT prototype, generated and provided by Qioptiq Photonics GmbH & Co. KG (see Figure 3).

For our measurements, we chose a representative scene of 1:30 minutes from each OR recording and placed the virtual site to the position where the real surgical site was in that specific recording. In order not to be biased by the choice of scene, we decided to use a scene in the middle of each recording, i.e. at exactly 2 hours after the start of the recording. Moreover, we discarded the first 10 seconds for warm-up of the Kalman and smoothing filter.

Finally, in the evaluation we examined how different parameters affect the lighting properties, which are (a) the parameter α presented in Section 3.4, which specifies the amount of simultaneous used light modules, (b) the score functions presented in Section 3.4, where 'OFF' represents no optimization and no response of the light modules to occluding geometry and (c) the usage on a flat wound (without a shadow casting tube) or a deep surgical site, see Figure 3.

4.2 Shadow reduction

First, we examined the average brightness and plotted it in Figure 4 as this indicates the amount of shadowing. The average brightness in the flat site with optimization is 56.2 klx - 59.2 klx depending on the setting (compared to 43.0 klx without optimization), which is very close to the expected optimum without shadows with about 57 - 62 klx depending on the position of the site (keep in mind that the preferred illumination of 80 klx refers just to the maximum value in the center of the site). Moreover, with the flat site, the settings regarding brightness have practically no impact.

However, in case of a deep site, our results show that they will be illuminated very low without optimization with an average of 11.4 klx – after all, the light from most lamps does not penetrate at all. While the brightness of both optimization scores is identical with $\alpha = 1.0$ and is 31.4 klx, since simply all available lamps are used, one sees that $s_{\text{Perpendicular}}$ with an average of 45.6 klx performs slightly better than $s_{\text{SuccessiveUnblocked}}$ with 39.4 klx, which might be explained

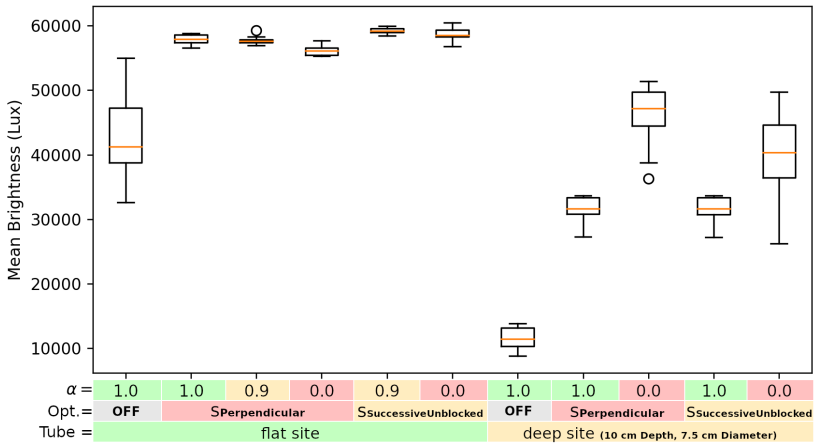

Fig. 4: Mean brightness: Brightness averaged over sensors and over time (n = 9 surgery sections).

by the fact that the light modules which can shine most vertically into the site and cause less shadows at the edge of the tube always tend to be selected.

4.3 Temporal Brightness Distribution

Comparing the brightness changes over time, it is noticeable that there are significantly more changes at the site without optimization than with activated optimization (see Fig. 5). However, except for a large $\alpha = 1.0$, where more changes occur over time than with $\alpha \leq 0.9$, the optimization settings have little effect on the overall rate of change when optimization is activated.

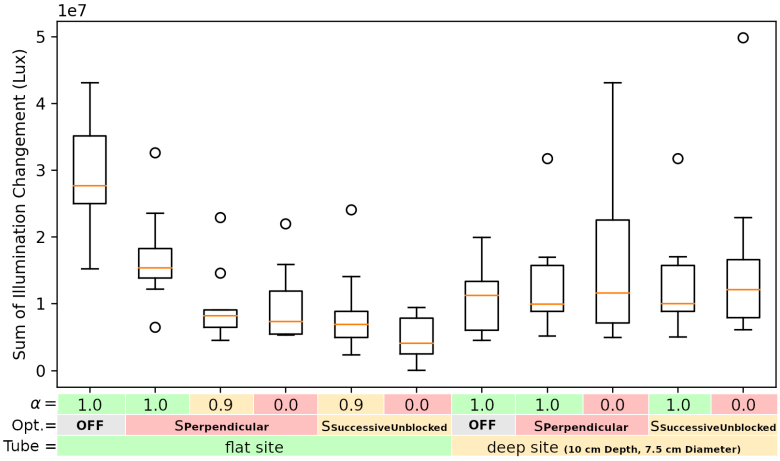

Fig. 5: Changes over time: Sum of illumination changes between adjacent frames, summed over all sensors (n = 9 surgery sections).

5 Conclusions and Future Works

We have presented a simple optimization algorithm for optimizing the illumination of a surgical site for new module-based lighting systems with a large number of swiveling automatically controlled light modules which are using depth sensors. We have investigated the influence of individual optimization parameters, namely, the number of simultaneously used lights and the depth of a virtual surgical wound with respect to the average brightness and changes in brightness. Finally, with our simulation, we were able to show that automatic optimization of intensity is a very effective means of preventing shadows and providing uniform illumination of the site over time.

In future work, we will evaluate the new lighting concept with the presented optimization within a real prototype and conduct a user study with active surgeons performing a task similar to actual operation. In this user study, we will also compare the performance to conventional SLS. Finally, we would like to consider the whole site *area* instead of only the site *center* for the optimization (see Section 3.4).

Acknowledgements

This work was partially funded by BMBF grant 13GW0264D.

References

[1] Arjan J Knulst et al. “Indicating shortcomings in surgical lighting systems”. en. In: *Minim Invasive Ther Allied Technol* 20.5 (Nov. 2010), pp. 267–275.

[2] Jahnavi Curlin and Charles K Herman. “Current State of Surgical Lighting”. en. In: *Surg J (N Y)* 6.2 (June 2020), e87–e97.

[3] Armin Dietz et al. “Contactless Surgery Light Control based on 3D Gesture Recognition”. In: *GCAI 2016. 2nd Global Conference on Artificial Intelligence*. Ed. by Christoph Benzmüller, Geoff Sutcliffe, and Raul Rojas. Vol. 41. EPiC Series in Computing. 2016, pp. 138–146.

[4] Jörn Teuber et al. “Autonomous Surgical Lamps”. In: *Jahrestagung der Deutschen Gesellschaft für Computer- und Roboterassistierte Chirurgie (CURAC)*. Bremen, Germany, Sept. 2015.

[5] Jörn Teuber et al. “Optimized Positioning of Autonomous Surgical Lamps”. In: *Proceedings of the SPIE Medical Imaging Conference*. Orlando, FL, United States of America: SPIE, Feb. 2017.

[6] Andre Mühlenbrock et al. “Optimizing the arrangement of fixed light modules in new autonomous surgical lighting systems”. In: *Medical Imaging 2022: Image-Guided Procedures, Robotic Interventions, and Modeling*. Ed. by Cristian A. Linte and Jeffrey H. Siewerdsen. Vol. 12034. International Society for Optics and Photonics. SPIE, 2022, pp. 491 –499.

[7] Andre Mühlenbrock et al. “Fast, accurate and robust registration of multiple depth sensors without need for RGB and IR images”. In: *The Visual Computer* (May 2022). ISSN: 1432-2315.